P9.7 Z_{DR} COLUMN CHARACTERISTICS AND TRENDS DURING THE 10 MAY 2010 SEVERE WEATHER OUTBREAK

Cynthia A. Van Den Broeke*, Clark D. Payne, and Les R. Lemon
Cooperative Institute for Mesoscale Meteorological Studies, The University of Oklahoma
NOAA/NWS Warning Decision Training Branch, Norman, Oklahoma

Paul T. Schlatter
NOAA/NWS Warning Decision Training Branch, Norman, Oklahoma

1. INTRODUCTION

With the imminent upgrade of the WSR-88D network to dual-polarization technology, forecasters in the National Weather Service (NWS) will have three new base variables. These new variables will allow analysis of dominant hydrometeor type in a given sample volume. The benefits of classifying dominant hydrometeor type may have direct application to warning decision making (i.e., real-time location of areas of hail or mixed-phase precipitation). With so much added information from the dual-pol variables, more research is needed on their direct operational applications.

One of the new base variables available with dual-polarization radar is differential reflectivity (Z_{DR}). Z_{DR} is the ratio of horizontal to vertical reflectivity, in dB, and can be expressed as:

$$Z_{DR} = Z_H - Z_V \quad (1)$$

where Z_H is horizontal reflectivity factor and Z_V is vertical reflectivity factor in dBZ. It follows that Z_{DR} is an indicator of shape and orientation of the dominant hydrometeor type in a sample volume. For example, oblate, horizontally-oriented rain drops will produce greater horizontal power return than vertical power return. The Z_{DR} in this scenario will be positive. For a hydrometeor with a vertically-oriented major axis, Z_V will be greater than Z_H, producing negative Z_{DR}. Finally, for hydrometeors that are nearly spherical or that have no preferred orientation, the ratio of Z_H to Z_V will be near 1, so Z_{DR} will be near 0 dB.

This discussion will focus primarily on observations of the Z_{DR} columns of 10 May 2010, with an emphasis on operational implications of the signature. First, some background on Z_{DR} columns and the 10 May 2010 pre-storm environment are presented. The concluding sections cover observations of Z_{DR} columns and discussion of potential operational applications.

1.1 Z_{DR} Columns

The Z_{DR} column is an area of positive Z_{DR}, caused by the presence of liquid drops, above the environmental melting level (Brandes et al. 1995). Z_{DR} columns are closely associated with the storm updraft (Brandes et al. 1995, Conway and Zrnic 1993). The cross section through the updraft of a severe convective storm in (Fig.1) is an example of a Z_{DR} column. The melting layer is clearly visible as the transition from values near 0 dB aloft to strongly positive values of Z_{DR} closer to the surface. The Z_{DR} column is the area of strongly positive Z_{DR} extending well above the melting layer into the area dominated by near-zero values.

With such a close association of the Z_{DR} column with updraft, it follows that this signature may have some value in warning decision making. Scharfenberg et al. (2004) suggest the possibility of anticipating short-term convective evolution based on Z_{DR} column characteristics. Picca and Ryzhkov (2010) indicate some potential use of the Z_{DR} column in short-term forecasting of hail growth.

**Corresponding author address:* Cynthia A. Van Den Broeke, 120 David L. Boren Blvd., Suite 2640, Norman, OK 73072; e-mail: Cynthia.vandenbroeke@noaa.gov

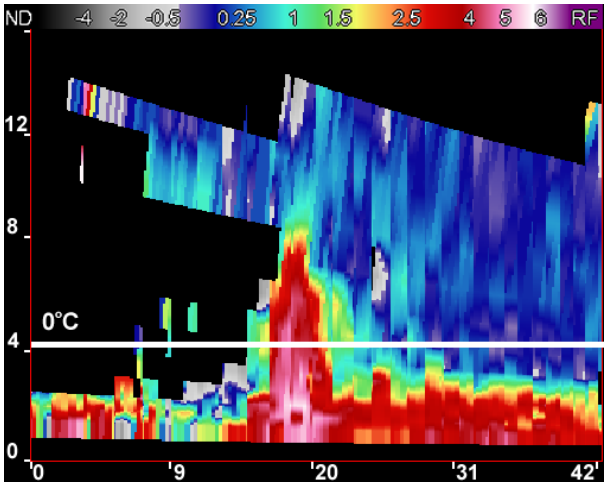

Figure 1. Z_{DR} cross section through the updraft of a convective storm. Horizontal, bold white line marks the approximate location of the 0°C isotherm. Distances on axes are in km. Strongly positive values of Z_{DR} are in reds and yellows, and dark blue is near 0 dB.

1.2 10 May 2010 Pre-storm Environment

On 10 May 2010, the pre-storm environment in central Oklahoma was characterized by high shear and high instability. Low-level moisture advection ahead of an approaching dryline resulted in dewpoint temperatures near or in excess of 20°C by 2100 UTC (Fig. 2). Low-level

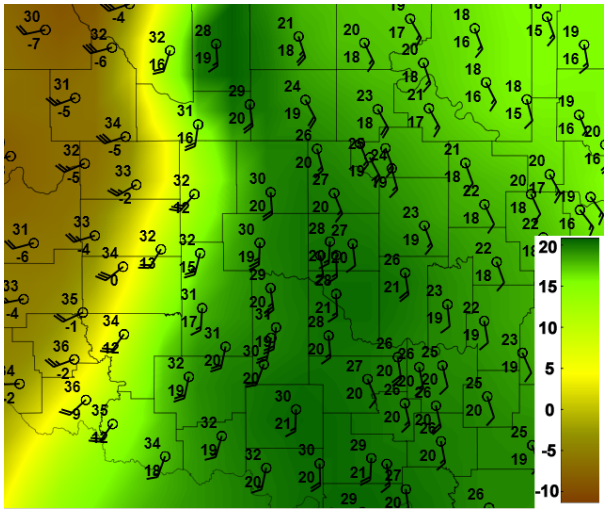

Figure 2. Low level wind (a full barb represents 5 m/s), temperature (top left) and dewpoint (bottom left) in °C. for central Oklahoma on 10 May 2010 at 2100 UTC. Color gradient represents dewpoint in °C. Strong gradient in dewpoint temperature in west-central Oklahoma is an approaching dryline.

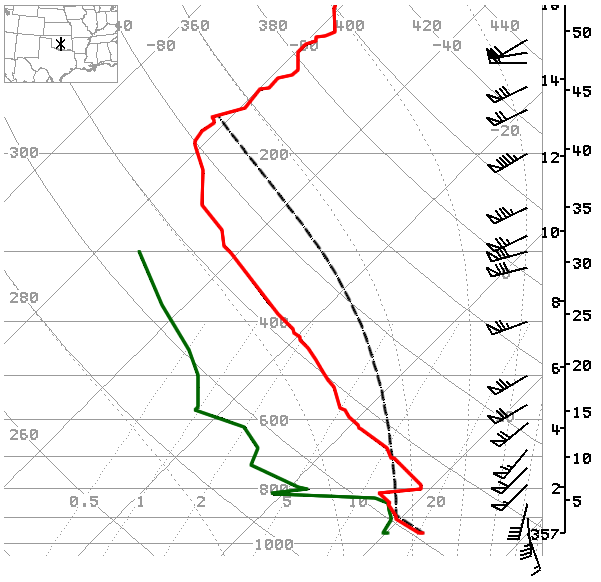

Figure 3. 10 May 2010 2100 UTC sounding taken from Norman, Oklahoma (KOUN). Numbers to the left of the vertical staff on the right side of the sounding are in km. Temperature is in red and dewpoint temperature in green

flow was southerly ahead of the dryline, with some convergence at the surface near the dryline. Upper-level flow was heavily influenced by a short-wave trough approaching from the west, with flow mostly westerly or southwesterly ahead of the trough (Fig 3). The 2100 UTC sounding taken from KOUN shows both strong directional and speed shear in the lowest 6 km, with backed low-level flow at the surface (Fig. 4). Despite the cap between 700 and 800 hPa, there was very strong instability present, with CAPE exceeding 3000 J kg^{-1}.

2. DATA

Dual-polarization data from 10 May 2010 were collected using KOUN, a test WSR-88D dual-polarization radar in Norman, Oklahoma. The data on 10 May were still considered test data, and therefore subject to potentially lower data quality. For this event, the Z_{DR} was not fully calibrated when convective initiation took place, leading to values a few tenths of a dB too low. These data were corrected by 0.35 dB to reflect expected values of Z_{DR} in dry snow and drizzle.

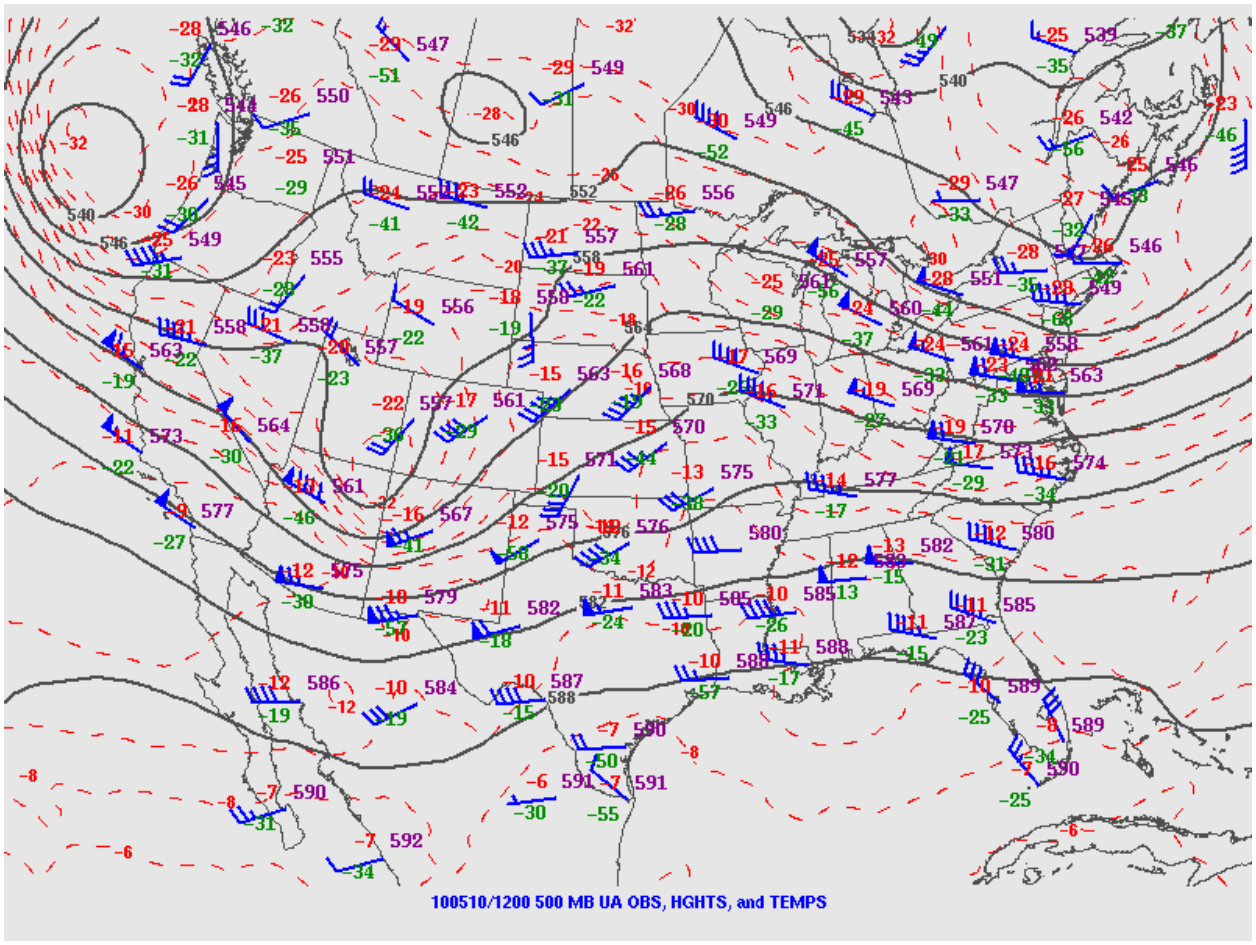

Figure 4. 1200 UTC 500 hPa analysis from 10 May 2010. Courtesy Storm Prediction Center (www.spc.noaa.gov).

Data collection began at 2041 UTC with convection well underway in north-central Oklahoma. The event lasted through just after 0200 UTC on the 11th. Data were collected using VCP 12 which has 14 elevation angles and a volume scan update time of approximately 4.5 minutes.

Radar data were compared with hourly surface observations and the 2100 UTC KOUN sounding. The proximity of the sounding, both spatially and temporally, to many of the supercells was helpful for evaluation of the thermal profile of the near-storm environment. Comparison with storm reports was done using Storm Data.

3. METHODOLOGY

To apply the Z_{DR} column to warning decision making, only software available to a NWS forecaster in an operational environment was used for analysis. The primary tools for analysis were the Advanced Weather Interactive Processing System (AWIPS) and the Four-Dimensional Stormcell Investigator (FSI). In AWIPS it is relatively straightforward to analyze environmental data alongside of the radar data. FSI allows for flexible analysis of cross sections and CAPPIs.

Z_{DR} columns were identified as areas of Z_{DR} exceeding 1.5 dB that extended above the environmental 0°C level. On 10 May 2010, the environmental 0°C level was at approximately 4.2 km mean sea level (MSL). To exclude potential radar artifacts or spurious positive values of Z_{DR}, there must have been vertical continuity between elevation angles for positive Z_{DR} values to be considered part of the Z_{DR} column. Data quality checks were also performed using correlation

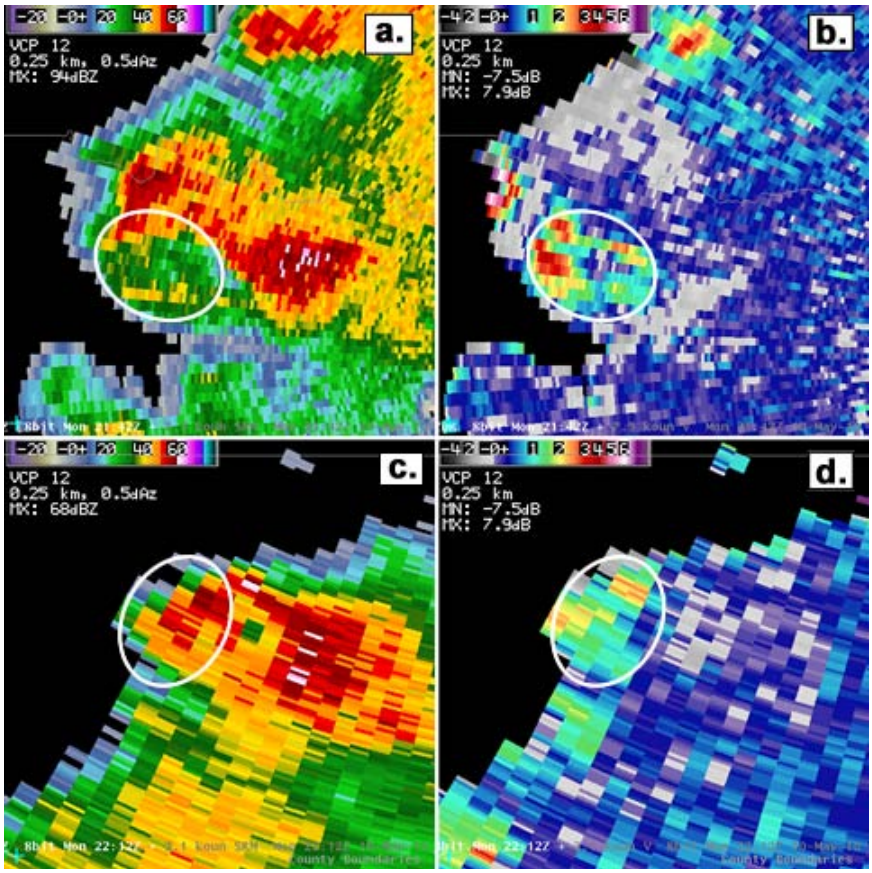

Figure 5. a) 2142 UTC reflectivity image of a supercell at the 8.0° elevation angle with a white circle marking the location of the Z_{DR} column. b) Z_{DR} at the same elevation and time as in (a). White circle denotes Z_{DR} column. c) 2212 UTC reflectivity image at the 3.1° elevation angle with white circle showing the location of the Z_{DR} column. d) Z_{DR} image corresponding to c) with Z_{DR} column denoted by the white circle.

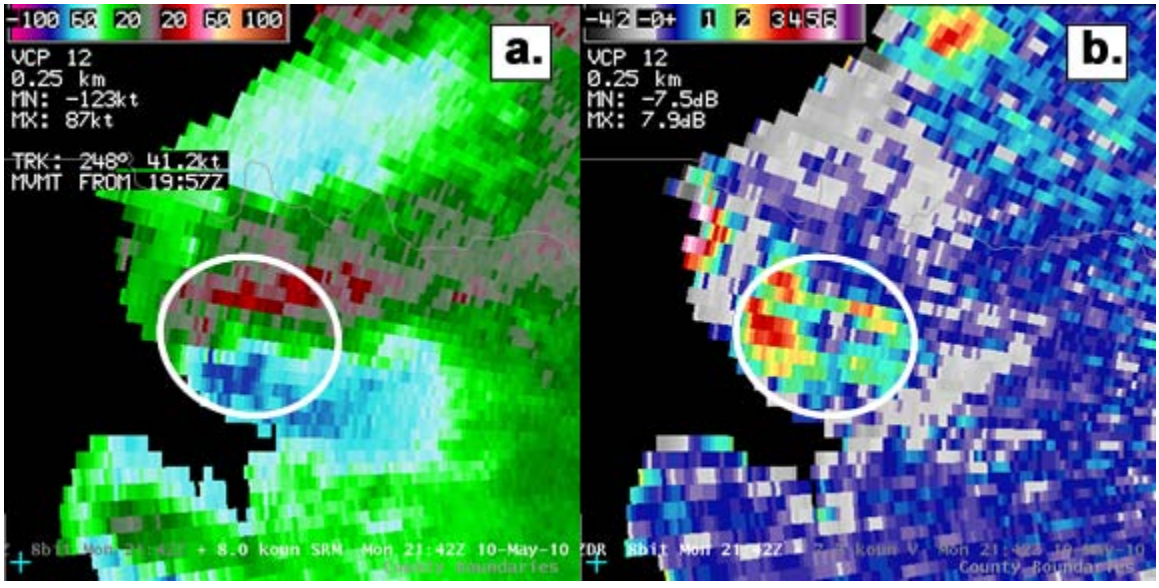

Figure 6. a) 2142 UTC SRM at 8.0 with white circle at the location of the ZDR column. b) ZDR column at same time and elevation as in a).

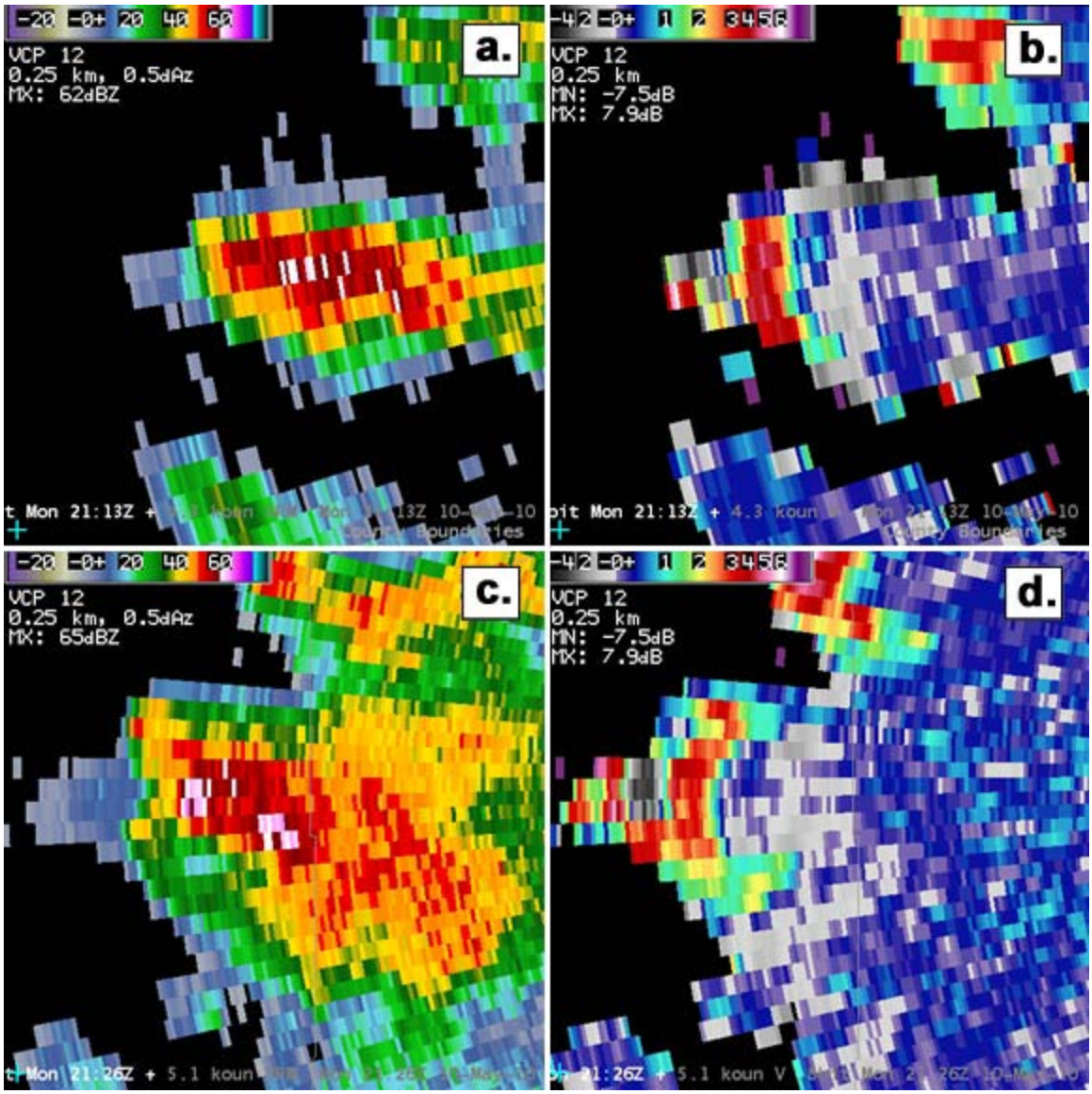

Figure 7. a) 2113 UTC reflectivity of convective storm at 4.3° elevation angle during early lifecycle. b) Z_{DR} at same elevation angle and time as in a). Height is approximately 6.8 km MSL. c) Reflectivity of convective storm at 2126 UTC, after BWER development. Elevation angle is 5.1°. d) Z_{DR} for same time and elevation as in c). Height approximately 6.6 km MSL.

coefficient (CC) and spectrum width to eliminate contribution by three-body scattering.

Each storm was monitored from shortly after first echo until the last Z_{DR} column had dissipated, or until the storm had moved beyond 135 km from the radar. The location of each Z_{DR} column with respect to the mid-level mesocyclone, BWER, reflectivity core, and tornado (if applicable) were recorded. Changes in the location or number of Z_{DR} columns were noted. If a new Z_{DR} column developed, it was tracked separately. The storms examined include five right-moving supercells (four were tornadic) and two anticyclonic, tornadic left-moving supercells.

4. RESULTS

In mature supercells, the Z_{DR} column was often closely, though not universally, associated with some type of inflow feature such as a Weak Echo Region (WER) or a Bounded Weak Echo Region (BWER). When this was the case, the Z_{DR} column was slightly offset to the upshear side of the center of the WER or BWER (Fig. 5a, b).

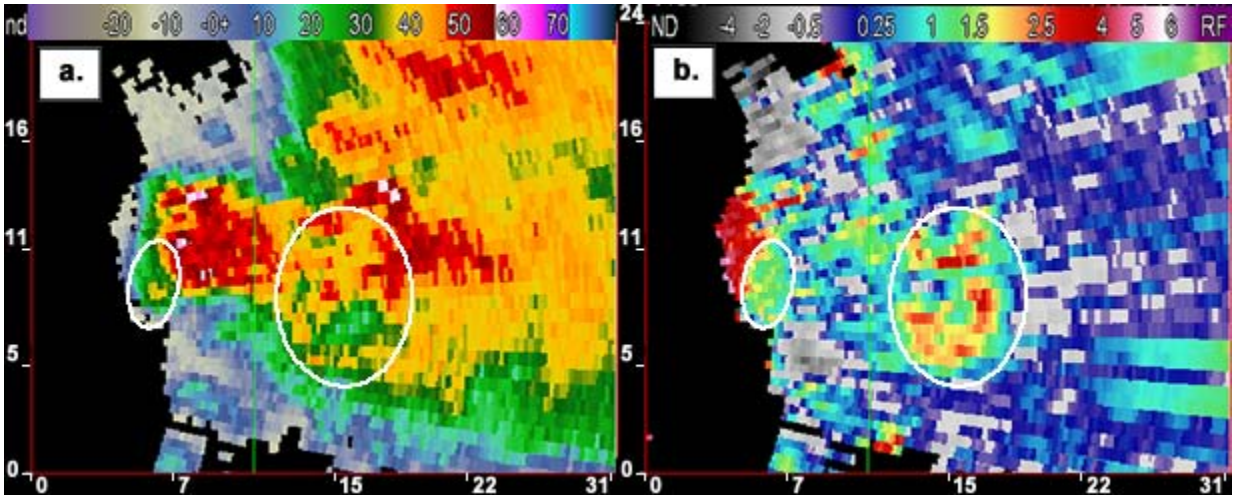

Figure 8. a) CAPPI of reflectivity at 6.1 km MSL at 2245 UTC. Location of the Z_{DR} columns indicated by white circles. b) CAPPI of Z_{DR} at the same time and height as in a).

Hubbert et al. (1998) also observed some offset between the Z_{DR} column and the WER in their case. The Z_{DR} column of the left-moving supercell also briefly held this appearance (Fig. 5c, d). With respect to the mid-level mesocyclone in the right-moving supercells, the Z_{DR} column was either colocated or slightly offset from the center toward the south or southwest (Fig. 6).

With respect to storm maturity, there were some changes in Z_{DR} column characteristics from just after first echo through the time the storm first showed supercell characteristics. The changes varied slightly on a storm by storm basis, but had some similarities. The most striking changes took place in a short-lived, right-moving supercell. The Z_{DR} column during the early life of this storm was characterized by extremely high values greater than 3.5 dB through most of its depth (Fig. 7a, b). As the storm matured and developed a BWER, Z_{DR} dropped below 3.5 dB in most of the column (Fig. 7c, d). The southern portion of the column, most closely associated with the newly-developed BWER, had the lowest values of Z_{DR}. The reason for this transition is unknown, but one possible cause may be the development of a new updraft pulse.

Not many of the observed supercells went through a cycling process within a 135 km radius of the radar. In fact, most storms observed experienced interference from nearby convection and subsequent demise before cycling took place. Exceptions include one right-moving supercell and one left-moving supercell. Unfortunately, during the cycling process of the right-moving supercell, a test was done on the radar, causing a substantial delay in the volume scan update and compromising the data quality of some tilts of the next volume scan at 2245 UTC. This volume scan was still useful if the data were interpreted with caution. A CAPPI taken at 6.1 km at 2245 UTC on a tornadic supercell east of KOUN showed multiple Z_{DR} columns. Column 1 was on the extreme western fringe of the storm. The reflectivity core associated with the first column appeared to be separate from that associated with column 2. Column 2 was also associated with a BWER. Without better temporal continuity, it was difficult to ascertain if this was indeed part of the cycling process.

The cycling process was much more evident in one of the left-moving supercells. At 2212 UTC, a view of the mid-levels showed a Z_{DR} column removed to the west of the main BWER and mesoanticyclone (Fig. 9a-c). By 2216 UTC, the Z_{DR} column had broadened noticeably (Fig 9d, e). At 2221 UTC, the column had two distinct maxima in Z_{DR} (Fig. 9g, h). The westernmost maximum cp appeared to be the “old” Z_{DR} column, while the second maximum was associated with development of a new WER (not shown) and an enhancement in storm-relative inbound flow (Fig.

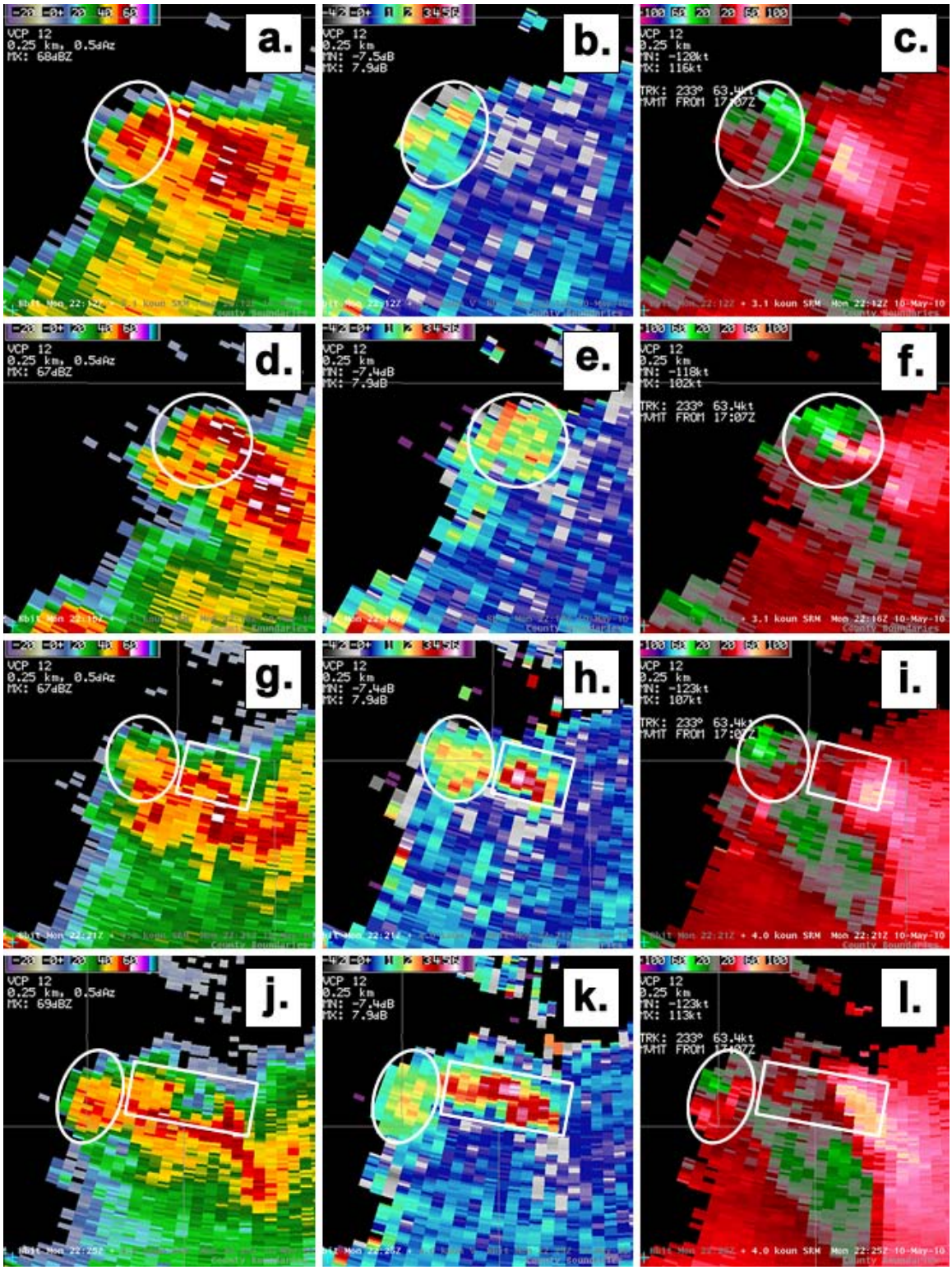

Figure 9. Reflectivity (a), Z_{DR} (b), and SRM (c) for a left-moving supercell at 3.1 (5.1 km MSL) at 2212 UTC. Circle indicates location of the Z_{DR} column at this time. d-f) As in a-c, except height is 4.6 km MSL at 2216 UTC. g-i) As for a-c, except at 2221 UTC for at a height of 5.1 km MSL and elevation angle of 4.0. j-l) As in g-i, except time is 2225 UTC and height is 4.8 km MSL.

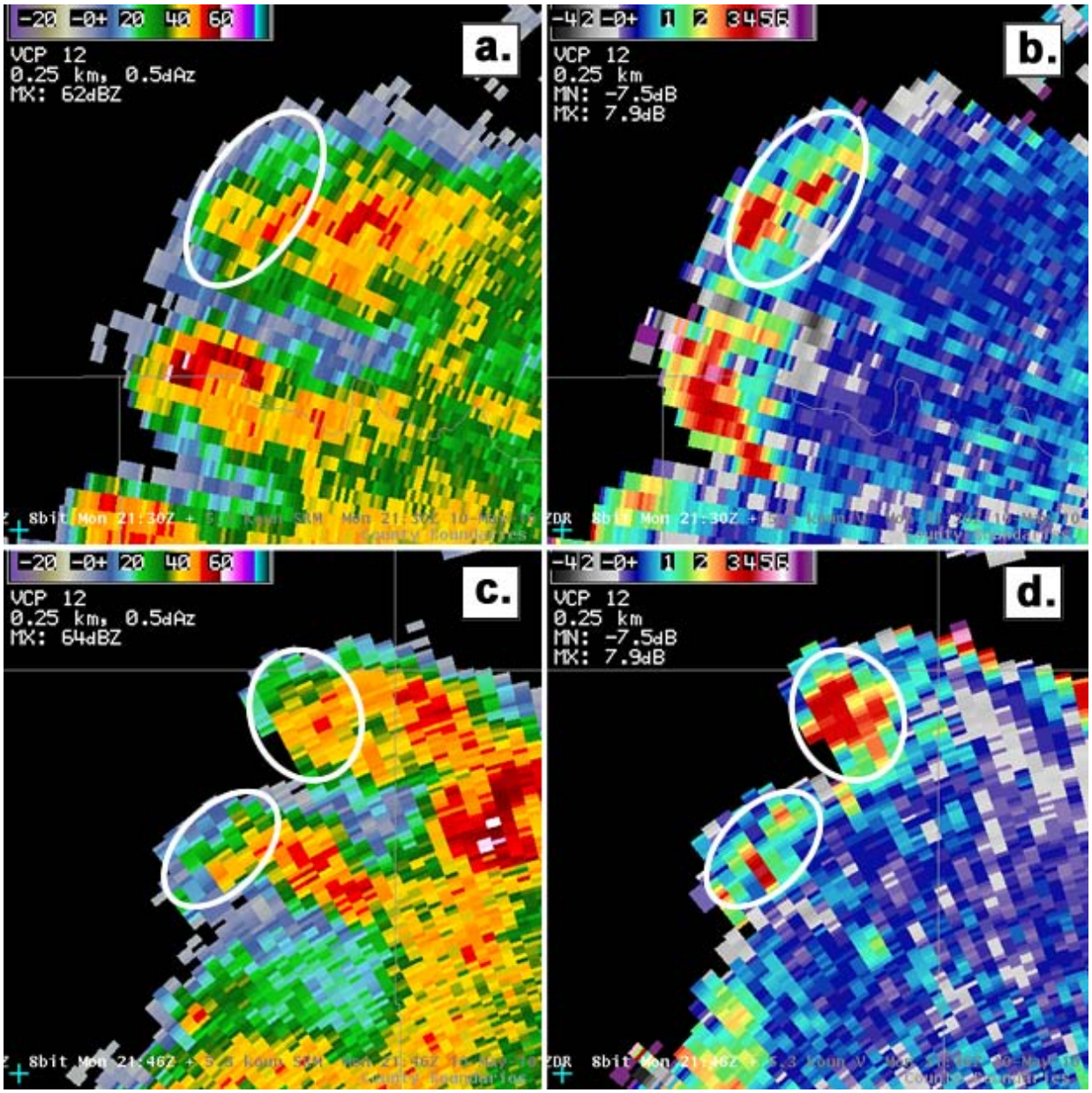

Figure 10. a) 2130 UTC reflectivity at the 5.1° elevation angle. Location of ZDR column indicated by the white circle. b) ZDR product corresponding to a). c) 2146 UTC reflectivity image at the 5.1° elevation angle. Locations of ZDR columns indicated by white circles. d) ZDR image corresponding to c).

9i). Unexpectedly, the Z_{DR} values in this new column were much higher than those with the old Z_{DR} column. Finally, at 2225 UTC, a new BWER developed in association with the new updraft pulse (Fig. 9j, k). Storm-relative inbound flow also increased at the same elevation angle, perhaps signifying the development of a new mesoanticyclone (Fig. 9l). Values of Z_{DR} within the new column remained much higher than in the old column, suggesting the new Z_{DR} column may have had a drop size distribution dominated by larger drops.

Occasionally the appearance of a new updraft signified that the storm was in the process of splitting. Both left-moving supercells exhibited the tendency to split, with one splitting multiple times. In Figure 10a, at 2130 UTC, the storm of interest had already split once. The Z_{DR} column of the northernmost member had an elongated appearance (Fig. 10b). In fact, there are 2 separate maxima in Z_{DR}. By 2146 UTC, the storm

had split, as evidenced in the reflectivity image at 5.1° elevation angle (Fig. 10c). In Z_{DR}, each storm had its own Z_{DR} column, with the left-moving member having the larger of the two columns (Fig. 10d).

5. DISCUSSION

The Z_{DR} column, when used with knowledge of storm structure in the traditional base moments (reflectivity, velocity, and spectrum width), may be helpful in determining the onset of storm cycling in some cases. Although it is not likely that better determining occurrence of storm cycling would directly impact warning metrics at this time, it could be another tool for generally situational awareness of storm morphology.

Anticipating storm splitting can be very important in the context of warning decision making. In the event of a split, one or both members of the split may be prone to leaving an existing warning polygon. Anticipating the split could lead to a change in warning polygon strategy. For all potential applications, it is emphasized that these observations are from a single, high-instability, high-shear event. These observations may not be applicable in all cases and future research should focus on repeatability of these observations.

ACKNOWLEDGMENTS

This extended abstract was prepared by Cynthia Van Den Broeke, Clark Payne, Les Lemon, and Paul Schlatter with funding provided by the NOAA/Office of Oceanic and Atmospheric Research under NOAA-University of Oklahoma Cooperative Agreement #NA17RJ1227, U.S. Department of Commerce. The statements, findings, conclusions, and recommendations are those of the authors and do not necessarily reflect the views of NOAA or the U.S. Department of Commerce.

REFERENCES

Brandes, E. A., J. Vivekanandan, J. D. Tuttle, and C. J. Kessinger, 1995: A study of thunderstorm microphysics with multiparameter radar and aircraft observations. *Mon. Wea. Rev.*, **123**, 3129-3143.

Conway, J. W., and D. S. Zrnic, 1993: A study of embryo production and hail growth using dual-Doppler and multiparameter radars. *Mon. Wea. Rev.*, **121**, 2511-2528.

Hubbert, J., V. N. Bringi, L. D. Carey, and S. Bolen, 1998: CSU-CHILL polarimetric radar measurements from a severe hail storm in eastern Colorado. *J. Appl. Meteor.*, **37**, 749-775.

Picca, J. C., and A. V. Ryzhkov, 2010: Polarimetric signatures of melting hail at S and C bands: detection and short-term forecast. *26th Conf. on Interactive Information and Processing Systems for Meteorology, Oceanography, and Hydrology*, Atlanta, GA, Amer. Meteor. Soc. Available: http://ams.confex.com/ams/pdfpapers/161240.pdf

Scharfenberg, K. A., P. T. Schlatter, D. J. Miller, and C. A. Whittier, 2004: The use of the "Z_{dr} column" signature in short-term thunderstorm forecasts. *11th Conf. on Av. Range and Aerospace Meteor.*, Hyannis, MA, Amer. Meteor. Soc. Available: http://ams.confex.com/ams/pdfpapers/81805.pdf